

# **0.7 % magnetic field induced strain in polycrystalline Ni<sub>50</sub>Mn<sub>29</sub>Ga<sub>21</sub> ferromagnetic shape memory alloy**

A. Satish Kumar<sup>1\*</sup> and V. Seshubai<sup>2</sup>

Lecturer, Dept. of Physics, Rajiv Gandhi University of Knowledge and Technology, Nuzvid-521201, India<sup>1</sup>

Professor, School of Physics, University of Hyderabad, Central University P.O., Hyderabad – 500046, India<sup>2</sup>

**Abstract:** Structural, microstructural and magnetic properties of polycrystalline Ni<sub>50</sub>Mn<sub>29</sub>Ga<sub>21</sub> alloy are studied. Processing parameters are optimized to get large grain size and multimode twinning in polycrystalline alloy. The polycrystalline alloy shows significantly low detwinning stress of 19 MPa and high magnetic field induced strain of 0.7%. Presence of large grain size with multimode twinning, 7M modulated crystal structure, large magnetocrystalline anisotropy and high saturation magnetization are key factors for observation of large magnetic field induced strain in polycrystalline alloy.

**Keywords:** : Ferromagnetic shape memory alloys, Magnetic field induced strain, Grain size, Low detwinning stresses.

## **I. INTRODUCTION**

In the recent years, the single crystals of Ni-Mn-Ga ferromagnetic Heusler alloys have attracted a great deal of attention owing to their ability to exhibit large magnetic field induced strain (MFIS) [1]. The large MFIS is due to the rearrangement of twin variants in the martensite by an applied magnetic field leading to an overall change of shape. The main thermodynamic driving force for twin boundary motion in the presence of a magnetic field is the high magnetocrystalline anisotropy of the low-symmetry martensitic phase [2, 3]. Low twin boundary energy, high magnetocrystalline anisotropy energy, high saturation magnetization and modulated crystal structure are some of the key factors for large magnetic field induced strain [3-5].

The off-stoichiometric Ni-Mn-Ga alloys crystallize in various structures depending on composition and thermo-mechanical treatments. In the austenitic phase, Ni<sub>2</sub>MnGa compound has L2<sub>1</sub> atomic order, cubic structure with *Fm* $\bar{3}$ *m* space group [6]. The crystal structure of the martensitic phases in the above system has been reported to be tetragonal or monoclinic with five layered modulation (5M) [7], orthorhombic or monoclinic with seven layered modulation (7M) [8, 9] or non-modulated tetragonal (NM) [6]. Among the martensitic phases, large magnetic-field-induced strain (MFIS) of 6% and 10% respectively have been reported in the 5M and 7M structures at considerably low stresses [1]. The stress levels required to cause considerable strain are very high in NM structures [10].

Among the off-stoichiometric compositions reported in the Ni-Mn-Ga system, Ni<sub>50</sub>Mn<sub>29</sub>Ga<sub>21</sub> with 7M orthorhombic crystal structure has been widely studied as it exhibits a large strain of 10 % in single crystals which is induced either by magnetic fields of the order of 1T or by low uniaxial stresses of nearly 2 MPa [3]. Such large strain arises from high magneto-crystalline anisotropy and low detwinning stresses caused by modulated crystal structure in martensitic phase [1, 3]. On the other hand, at 50 MPa uniaxial stresses, stress induced strains of less than 1% is reported [11], before training and 8% after training in the Ni<sub>50</sub>Mn<sub>29</sub>Ga<sub>21</sub> textured alloys in martensitic state. The MFIS value reported in textured Ni<sub>50</sub>Mn<sub>29</sub>Ga<sub>21</sub> is ~1 % [12]. The highest value of MFIS achieved so far in polycrystalline state has been 0.3 % in Ni<sub>49.6</sub>Mn<sub>28.4</sub>Ga<sub>22</sub> alloy [13] but it crystallizes in multi-phase. Recently we have reported [14] considerable compressive strain of the order of 5% with 1.8% residual strain and 89% recovery ratio after 124 MPa stress is applied in a Ni<sub>53.5</sub>Mn<sub>26</sub>Ga<sub>20.5</sub> composition. This was shown to have its origin in the low stresses, arising from a transformation from Cubic austenite to a martensite with modulated monoclinic structure, and the associated multimode twinning.

The physical properties of Ni-Mn-Ga alloys are very sensitive to the processing conditions and composition [15-18]. The heat treatments of these alloys strongly influence the structure and physical properties of these alloys [19]. The

# International Journal of Innovative Research in Science, Engineering and Technology

(An ISO 3297: 2007 Certified Organization)

Vol. 2, Issue 9, September 2013

strain induced due to magnetic field or load (stress) application depends on the grain size, crystal structure and the crystallographic orientation of the Ni-Mn-Ga alloys. Even though the oriented crystals (single crystals and textured alloys) with modulated crystal structure exhibit large strain levels at low stresses [3, 12], the preparation of single crystal or textured alloys is too involved for large-scale applications.

In this context, optimizing the properties of polycrystalline specimen through process modifications is of importance. In this paper, we accommodated different processing conditions for preparation of polycrystalline alloy.

## II. EXPERIMENTAL

An ingot of Ni-Mn-Ga with a initial composition  $\text{Ni}_{50}\text{Mn}_{29}\text{Ga}_{21}$  (in at.%) was prepared using induction melting of appropriate quantities of the constituent elements Ni (99.999%), Mn (99.99%) and Ga (99.999%) in an argon atmosphere. 1.2 wt.% excess of Mn over initial composition was added to compensate for the evaporation of Mn during the process. Melting points of the alloys were determined using a Mettler Toledo DTA1 facility. The ingot was sealed in high purity double quartz tube (i.e. the quartz tube with ingot was sealed in another high pure quartz tube) under argon atmosphere and heated up to 1200 °C in the vertical furnace. The temperature of vertical furnace was reduced at a rate of 5 °C per minute up to 830 °C, followed by water quenching. For better homogenization, the ingot alloy was further annealed at 830 °C for 8 days under vacuum in quartz ampoules. After 8 days annealing the ingot was quenched into ice water, following procedures described in the literature [20]. The composition of the alloy was determined to be  $\text{Ni}_{49.8}\text{Mn}_{29.1}\text{Ga}_{21.1}$  (in at.%) using wavelength dispersive spectrometry (WD). The martensitic transformation temperatures as well as the Curie temperatures were determined from both Differential Scanning Calorimetry (DSC), using a Mettler Toledo DSC1 equipment operated in the temperature range 150 to 873 K and low field ac magnetic susceptibility measurement carried out at 33 Hz frequency in the temperature range 200- 430 K. Small portion of the bulk sample was powdered and annealed under inert atmosphere at 500 °C for 12h and was furnace cooled, to remove the residual stresses incorporated due to crushing. The crystal structures at ambient temperature were determined from the X-ray diffraction patterns recorded in the ribbon and the annealed powder of the bulk sample, using a Philips X'pert X-ray Diffractometer with  $\text{Cu K}\alpha$  radiation. The data were collected using step scan with step size  $\Delta 2\theta = 0.02^\circ$  and scan rate of 10 sec per step. The magnetic isotherms (M-H curves) were recorded using a Vibrating Sample Magnetometer (VSM) facility on PPMS of Quantum design make. A Cylindrical rods with dimensions  $\text{Ø } 5.6 \text{ mm} \times 12 \text{ mm}$  were cut, using an electro discharge machine, from the bulk polycrystalline rod sample for carrying out stress-induced and magnetic field-induced strain measurements. Compressive stress-strain measurement was performed at room temperature on an INSTRON 5500R MTS at a crosshead speed of 0.02 mm/min. MFIS measurements were performed up to 0.7 T field on a homemade setup employing a laser displacement sensor that measures the change in sample dimensions to 2  $\mu\text{m}$  sensitivity.

## III. RESULTS AND DISCUSSION

DSC measurements were performed to determine the transformation temperatures of the studied alloy. The DSC thermogram on heating and cooling of the alloy, in the temperature interval 200 - 400 K is shown in Figure 1(a). The characteristic transformation temperatures, i. e. martensitic start ( $M_s$ ), martensitic finish ( $M_f$ ), austenite start ( $A_s$ ), austenite finish ( $A_f$ ) and the Curie temperature ( $T_C$ ) are found to be 324 K, 305 K, 315 K, 336 K and 374 K respectively. The martensitic transformation temperature  $T_M$  defined as  $(M_s + M_f + A_s + A_f)/4$  is calculated to be 320 K. A thermal hysteresis is observed at the transition. The enthalpy and entropy changes at the martensitic transformation obtained from DSC Curves are calculated to be  $\Delta H = 5.28 \text{ J/g}$  and  $\Delta S = .017 \text{ J/g.K}$  respectively. The mean value between the exchange heat on the forward and reverse martensitic transformation temperatures (heating and cooling runs, respectively) was taken as  $\Delta H$ , while the entropy change was calculated as  $\Delta S = \Delta H / T_M$ . Due to the small signals on DSC curves, the Curie temperature was confirmed by ac susceptibility measurement. The characteristic transformation temperatures determined by ac susceptibility are nearly equal to the values obtained from DSC measurement, the values are presented in table 1.

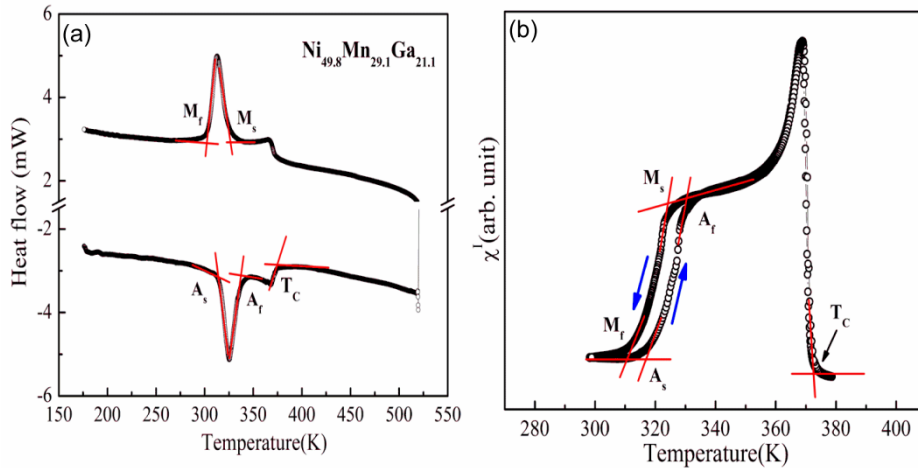


**Figure 1.** (a) DSC scans recorded while heating and cooling the alloy. The characteristic temperatures associated with the martensitic transformation, viz. martensitic start ( $M_s$ ), martensitic finish ( $M_f$ ), austenite start ( $A_s$ ) and austenite finish ( $A_f$ ), and the Curie temperature ( $T_C$ ) are indicated in the figure. (b) Temperature dependence of ac susceptibility recorded in the alloy during heating ( $\uparrow$ ) and cooling ( $\downarrow$ ).

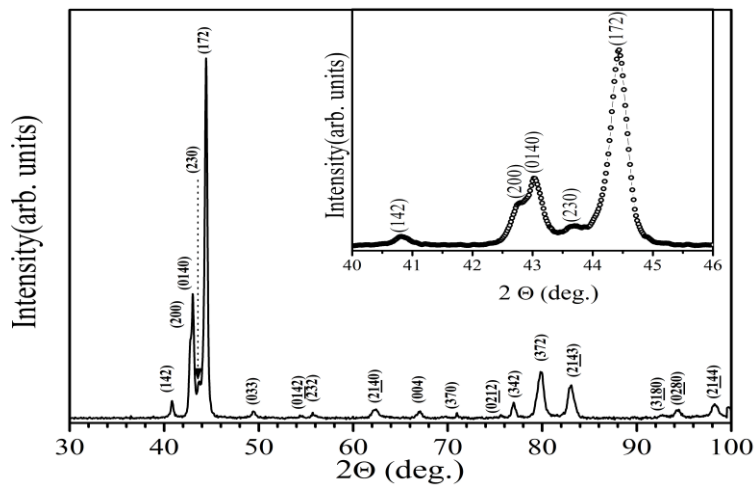


**Figure 2.** Powder X-ray diffraction (XRD) patterns of alloy indexed to 7 M- orthorhombic crystal structures at room temperature. The lattice parameters are computed to be  $a = 4.208(2) \text{ \AA}$ ,  $b = 29.371(1) \text{ \AA}$  and  $c = 5.588(9) \text{ \AA}$ . The inset shows the region  $40-46$  of  $2\theta(^{\circ})$ : reflection are labeled with Miller indexes.

Figure 2 shows the room temperature XRD patterns of  $\text{Ni}_{50}\text{Mn}_{29}\text{Ga}_{21}$  alloy, which is in the martensitic state at room temperature. The XRD pattern exhibits an orthorhombic crystal structure ( $pnmm$  space group) with 7M modulation, and the lattice parameters are  $a = 4.208(2) \text{ \AA}$ ,  $b = 29.371(1) \text{ \AA}$  and  $c = 5.588(9) \text{ \AA}$ . The observed pattern and the unit cell parameters are in agreement with reports for this composition in literature [8]. No secondary phase was observed in the diffraction pattern. The inset of figure 2 shows the expanded region of XRD pattern in the  $2$ -theta region  $40^{\circ} - 50^{\circ}$ .

## International Journal of Innovative Research in Science, Engineering and Technology

(An ISO 3297: 2007 Certified Organization)

Vol. 2, Issue 9, September 2013

**Table 1:** Martensitic start ( $M_s$ ), martensitic finish ( $M_f$ ), austenite start ( $A_s$ ) and austenite finish ( $A_f$ ), martensitic transformation temperature ( $T_M = (M_s + M_f + A_s + A_f)/4$ ) and Curie temperature ( $T_C$ ) of  $Ni_{50}Mn_{29}Ga_{21}$  alloy

Measurement	$M_s$ (K)	$M_f$ (K)	$A_s$ (K)	$A_f$ (K)	$T_M$ (K)	$T_C$ (K)
ac susceptibility	324	310	317	330	320	373
DSC	324	305	315	336	320	373

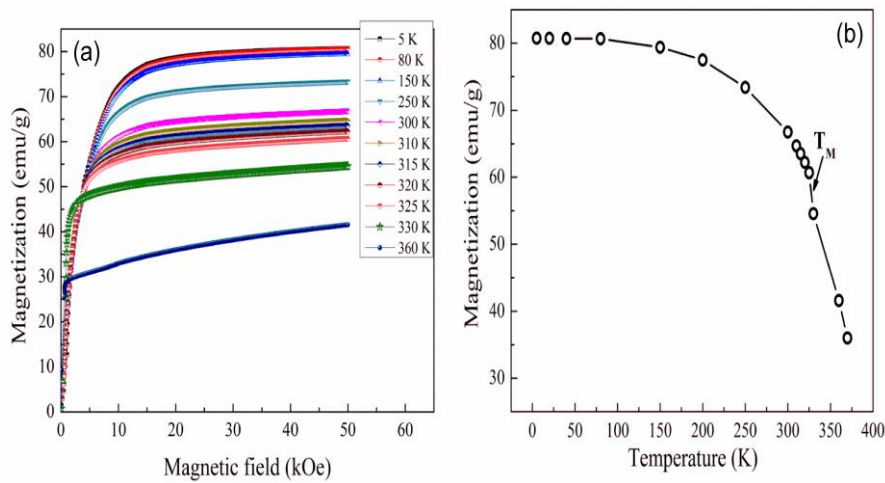


**Figure 3.** (Color online): (a) Magnetization as a function of magnetic field at selected temperature for  $Ni_{50}Mn_{29}Ga_{21}$  alloy. (b) Temperature dependencies of saturation magnetization of  $Ni_{50}Mn_{29}Ga_{21}$  alloy in the temperature interval 5 - 400 K.

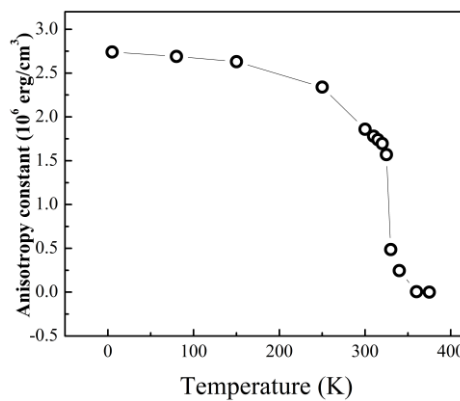


**Figure 4.** Temperature dependencies of Magnetocrystalline anisotropy constant  $K_1$  of  $Ni_{50}Mn_{29}Ga_{21}$  alloy in the temperature interval 5 - 400 K.

Magnetization versus magnetic field (M-H) measurements were made at different temperatures using VSM of the PPMS with a maximum applied field restricted to 5 Tesla. The saturation magnetization ( $M_{sat}$ ) was determined by approach to saturation method by plotting the magnetization (M) as a function of  $H^{-2}$  and extrapolating the linear high field region to infinite fields ( $H^{-2} \rightarrow 0$ ). The values of  $M_{sat}$  for different alloys are determined from the intercepts on magnetization-axis. The magnetization is observed to reach saturation at nearly two Tesla. The saturation magnetization values are found to be 81 emu/g and 66 emu/g at 5 K and 300 K respectively. The saturation magnetization as a

## International Journal of Innovative Research in Science, Engineering and Technology

(An ISO 3297: 2007 Certified Organization)

Vol. 2, Issue 9, September 2013

function of temperature during heating is shown in figure 3(b). The martensitic transformation is observed as a sudden reduction of saturation magnetization, which is indicated by an arrow in figure 3(b).

Albertini et al. [21] studied Compositional and temperature dependence of magnetic anisotropy of polycrystalline Ni-Mn-Ga alloys. They concluded that moving away from the stoichiometric composition, the magneto-crystalline anisotropy markedly affected by compositional changes and variation is more pronounced when Mn content is decreased. Figure 4 shows the temperature dependence of the magneto-crystalline anisotropy constant ( $K = H_A M/2$ ) of studied alloy. The singular point detection technique [22], which is a method for the measurement of the anisotropy field in polycrystalline specimen, was used to determine  $H_A$  of the polycrystalline alloy. The magneto-crystalline anisotropy constant at 300 K is found to be  $1.87 \times 10^6 \text{ erg/cm}^3$  and is comparable to the value reported in literature [21, 23].

Microstructure of a specimen plays an important role in deciding the mechanical properties of shape memory alloys [24, 25]. Zig-zag and/or herring-bone (saw-tooth) morphology is expected to be observed in the optical and electron microscopic studies when a growing martensitic variant impinges against a pre-existing variant. This is because the existing variant either stops growing at the impinged place, or it stimulates to produce a new variant with a different habit plane. It exhibits mostly straight-bands and occasional crossing of martensitic variants.

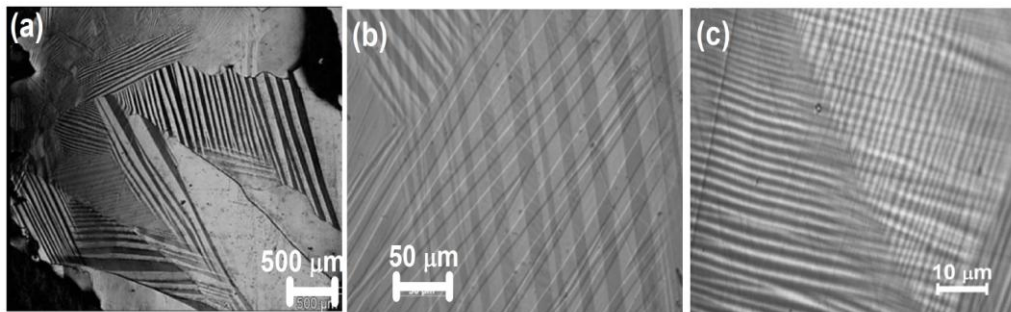


**Figure 5.** (a) Optical micrographs showing large grain size of the order of 1 mm and long range twin variants. (b) Shows abundance of parallel and crossing twin variants of ~ 20- 30  $\mu\text{m}$ . (c) Exhibits micro twinning at ~1 $\mu\text{m}$  size within the martensitic variants.

Figure 5 shows the optical microstructures recorded in polycrystalline specimens in the martensitic phase, after polishing down to 0.25  $\mu\text{m}$ . Parallel bands-like morphology and crossing of thermo-elastic martensite variants are spread over the entire sample indicating long-range deformation. The grain size of the bulk alloy is of the order of a millimeter as seen in the optical micrograph shown in Figure 5(a). Figure 5(a) and 5(b) displays abundance of parallel twin variants of ~20- 30  $\mu\text{m}$  widths as well as crossing of the variants as observed in the bulk sample. Figure 5(c) shows extensive micro-twinning within the martensitic variants in the bulk alloy. The multimode twinning is indicative of low residual stresses in the bulk sample.

Compressive stress-strain measurements carried out on the polycrystalline alloy is shown in Figure 6(a). The pseudo-elastic behaviour (i.e. the starting stress for twin variants reorientation) started at a stress level of about 19 MPa and corresponding strain levels observed to be 1.26%. However, the test was programmed to unload before the twin variants reorientation was completed. Therefore, the stress level to complete the reorientation was not determined. Nevertheless, the strain induced by twin variants reorientation was found to be 5.3% at 40 MPa. The stress value reported for producing similar strain in polycrystalline Ni-Mn-Ga alloys is of the order of 200 MPa [24] and is much higher compared to the present value. The low detwinning stress in present alloy can be attributed to the large grain size and multimode twinning in addition to the modulated crystal structure at room temperature.

It has been proven that, in a limited temperature range below the martensitic transformation temperature, it is possible to induce large strains in the martensitic phase, by the application of relatively low magnetic field [26]. Due to the increasing of detwinning stress with reducing temperatures, high fields are required to induce similar strain values well below martensitic transformation temperature. The magnetic field induced strain has been measured in the

# International Journal of Innovative Research in Science, Engineering and Technology

(An ISO 3297: 2007 Certified Organization)

Vol. 2, Issue 9, September 2013

polycrystalline rod at 300 K ( $T_M = 320\text{K}$ ). Pre-mechanical load of 20 MPa was applied along the long axis of the polycrystalline alloy to get detwined martensite. MFIS jumps from 0.06% to 0.64% as the magnetic field is increased above 4.8 kOe up to 5.0 kOe and is shown in Figure 6(b). On withdrawing the field, an irreversible magnetic field induced strain levels of 0.7% have been observed, which are higher than those reported so far in polycrystalline Ni-Mn-Ga alloys.

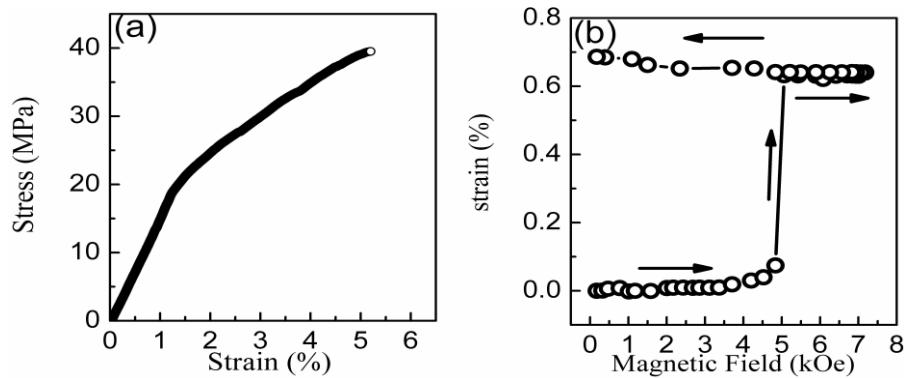


**Figure 6.** (a) Compressive stress - strain curve of bulk polycrystalline sample shows initial linear part of the curve terminating at 19 MPa and a strain of 1.26%, corresponds to the martensitic re-orientation stress and elastic strain respectively. (b) Magnetic field induced strain measured under a static compressive load of 1.3 MPa, applied perpendicular to magnetic field, on the polycrystalline rod specimen, showing a jump at 4.8 kOe and an irreversible MFIS of 0.7%.

We attribute the reason for the considerable strain levels thus observed at low detwinning stresses and the large MFIS obtained in the bulk sample of the present study to be due to the alteration in the processing conditions. We found this step to be crucial in forming large grains with 7M superstructural ordering exhibiting wide spread parallel and crossing twin variants within which micro-twinning takes place. Large magnetic anisotropy energy and high saturation magnetization, in addition to the close proximity to operation temperature and martensitic transformation temperature plays crucial role in exhibiting significant MFIS at lower fields.

## IV. CONCLUSIONS

The bulk polycrystalline alloy of the present composition exhibits an irreversible magnetic field induced strain of 0.7% on application of 5 kOe field, and a stress induced strain of 1.26% at 19 MPa which are higher than those reported so far in polycrystalline Ni-Mn-Ga alloys. Presence of large grain size with multimode twinning, 7M modulated crystal structure, large magnetocrystalline anisotropy, high saturation magnetization and close proximity of martensitic transformation temperatures to operating temperature are key factors for observation of large magnetic field induced strain in polycrystalline alloy. These results demonstrate the significant role played by the processing conditions in influencing the magnetic field induced strain in polycrystalline alloy.

## V. ACKNOWLEDGMENTS

Funding from ADA, Bangalore in the form of a project (Ref.No. ADA/AF/DISMAS/163/2005) is gratefully acknowledged. ASK thanks CSIR (Ref. No. 03 (1065) 106/EMR-II). The authors are thankful to DST-Centre for Nanotechnology for PPMS facility.

## REFERENCES

- [1] Ullakko, K., Huang, J.K., Kantner, C., R. C. O’Handley, R.C., Kokorin, V.V., “Large magnetic-field-induced strains in  $\text{Ni}_2\text{MnGa}$  single crystals”, *Appl. Phys. Lett.*, vol.69, pp. 1966-1968, 1996.
- [2] Murray, S.J., Marioni, M., Allen, S.M., O’Handley, R.C., Lograsso, T. A, “6% magnetic-field-induced strain by twin-boundary motion in ferromagnetic Ni-Mn-Ga”, *Appl. Phys. Lett.* Vol. 77, pp.886-888, 2000.

# International Journal of Innovative Research in Science, Engineering and Technology

(An ISO 3297: 2007 Certified Organization)

Vol. 2, Issue 9, September 2013

- [3] Sozinov, A., Likhachev, A. A., Lanska, N., Ullakko, K., "Giant magnetic-field-induced strain in NiMnGa seven-layered martensitic phase", Appl. Phys. Lett. Vol. 80, pp.1746-1748, 2002.
- [4] L'vov, V.A., Chernenko, V., "Magnetic Anisotropy of Ferromagnetic Martensites" Mater. Sci. Forum vol. 684, pp. 3147, 2011.
- [5] Karaca, H.E., Karaman, I., Basaran, B., Chumlyakov, Y.I., Maier, H.J., "Magnetic field and stress induced martensite reorientation in NiMnGa ferromagnetic shape memory alloy single crystals", Acta Mater., vol. 54, pp. 233-245, 2006.
- [6] Wedel, B., Suzuki, M., Murakami, Y., Wedel, C., Suzuki, T., Shindo, D., Itagaki, K., "Low temperature crystal structure of Ni-Mn-Ga alloys", J. Alloys Compd., vol. 290, pp.137-143, 1999.
- [7] Li, Z., Zhang, Y., Eshing, C., Zhao, X., Zuo, L., "Twin relationships of 5M modulated martensite in Ni-Mn-Ga alloy", Acta Mater. Vol. 59, pp. 3390-3397, 2011.
- [8] Ranjan, R., Banik, S., Barman, S. R., Kumar, U., Mukhopadhyay, P. k., Pandey, D., "Powder x-ray diffraction study of the thermoelastic martensitic transition in  $\text{Ni}_2\text{Mn}_{1.05}\text{Ga}_{0.95}$ ", Phys. Rev. B vol. 74, pp. 224443-224450, 2006.
- [9] Righi, L., Albertini, F., Villa, E., Paoluzi, A., Calestani, G., Chernenko, V., Besseghini, S., Ritter, C., Passaretti, F., "Crystal structure of 7M modulated Ni-Mn-Ga martensitic phase", Acta Mater., vol. 56, pp. 4529-4535, 2008.
- [10] Chernenko, V. A., Chmielus, M., Müllner, P., "Large magnetic-field-induced strains in Ni-Mn-Ga nonmodulated martensite", Appl. Phys. Lett., vol. 95, pp. 104103-104106, 2009.
- [11] Gaitzsch, U., Pötschke, M., Roth, S., Rellinghaus, B., Schultz, L., "Mechanical training of polycrystalline 7 M  $\text{Ni}_{50}\text{Mn}_{30}\text{Ga}_{20}$  magnetic shape memory alloy", Scripta Mater., vol.57, pp.493, 2007.
- [12] Gaitzsch, U., Pötschke, M., Roth, S., Rellinghaus, B., Schultz, L., "A 1% magnetostrain in polycrystalline 5M Ni-Mn-Ga" Acta Mater. Vol. 57, pp. 365, 2009.
- [13] Ullakko, K., Ezer, Y., Sozinov, A., Kimmel, G., Yakovenko, P., Lindroos, V. K., "Magnetic-field-induced strains in polycrystalline Ni-Mn-Ga at room temperature", Scripta mater., vol. 44, pp. 475-480, 2001.
- [14] Ramudu, M., Satish Kumar, A., Seshubai, V., Muraleedharan, K., Prasad, K.S., Rajasekharan, T., "Modulated monoclinic crystal structure and large shape memory effect in nickel-rich  $\text{Ni}_{53.5}\text{Mn}_{26.0}\text{Ga}_{20.5}$ ", Scripta Mater., vol. 63, 1073, 2010.
- [15] Cong, D.Y., Wang, Y.D., Zhao, X., Zuo, L., Lin Peng, R., Zetterström, P., Liaw, P.K., "Crystal structures and textures in the hot-forged Ni-Mn-Ga alloys", Metall. Mater. Trans. A, vol.37, pp.1397-1403, 2006.
- [16] Chernenko V.A., "Compositional instability of  $\beta$ - phase in Ni-Mn-Ga alloys", Scripta Mater. vol.40, pp-523-527, 1999.
- [17] Heczko, O., Straka, L., "Compositional dependence of structure, magnetization and magnetic anisotropy in Ni-Mn-Ga magnetic shape memory alloys", J. Magn. Mater. vol. 272-276, pp.2045-2046, 2004.
- [18] Chen, X.Q., Yang, F.J., Lu, X., Qin, Z.X., "The way composition affects martensitic transformation temperatures of Ni-Mn-Ga Heusler alloys", phys. stat. sol. (b), vol. 244, pp. 1047, 2007.
- [19] Gaitzsch, U., Pötschke, M., Roth, S., Mattern, N., Rellinghaus, B., Schultz, L., "Structure formation in martensitic  $\text{Ni}_{50}\text{Mn}_{30}\text{Ga}_{20}$  MSM alloy", J. Alloys Compd., vol. 443, pp. 99-104, 2007.
- [20] Vasil'ev, A. N., Bozhko, A. D., Khovailo, V.V., Dikshstein, I. E., Shavrov, V. G., Buchelnikov, V. D., Matsumoto, M., Suzuki, S., Takagi, T., Tani, J., "Structural and magnetic phase transitions in shape-memory alloys  $\text{Ni}_{1+x}\text{MnGa}_{1-x}$ ", Phys. Rev. B, vol. 59, pp. 1113 -1120, 1999.
- [21] Albertini, F., Pareti, L., Paoluzi, A., Morellon, L., Algarabel, P.A., Ibarra, M.R., Righi, L., "Composition and temperature dependence of the magnetocrystalline anisotropy in  $\text{Ni}_{2+x}\text{Mn}_{1+y}\text{Ga}_{1+z}$  ( $x+y+z=0$ ) Heusler alloys", Appl. Phys. Lett., vol. 81, pp. 4032-4034, 2002.
- [22] Asti, G., Rinaldi, S., "Singular points in the magnetization curve of a polycrystalline ferromagnet", J. Appl. Phys., vol. 45, pp.3600-3611, 1974.
- [23] Jiang, C., Muhammad, Y., Deng, L., Wu, W., Xu, H., "Composition dependence on the martensitic structures of the Mn-rich NiMnGa alloys", Acta Mater., vol. 52, pp. 2779, 2004.
- [24] Li, Y., Xin, Y., Jiang, C., Xu, H., "Shape memory effect of grain refined  $\text{Ni}_{54}\text{Mn}_{25}\text{Ga}_{21}$  alloy with high transformation temperature", Scripta Mater., vol. 51, pp. 849-852, 2004.
- [25] Dunand, D. C., Müllner, P., "Size Effects on Magnetic Actuation in Ni-Mn-Ga Shape-Memory Alloys". Adv. Mater., vol.23, pp. 216-232, 2011.
- [26] Farrell, S. P., Dunlap, R. A., Cheng, L. M., Ham-Su, R., Gharghoury M. A., Calvin V. Hyatt, C. V., "Magnetic properties of single crystals of Ni-Mn-Ga magnetic shape memory alloys", Proc. SPIE vol.5387, pp.186, 2004.